clearly indicates that a separate product is being formed.

Diimide formation has been confirmed chemically by observing the yield in the presence of coadsorbed hydrogen and coadsorbed oxygen with both hydrazine and ammonia on the Rh surface (Figure 4). In the presence of coadsorbed hydrogen, the yield of diimide increased substantially for both N_2H_4 and NH_3. In the presence of hydrogen, we propose that the concentration of NH(ad) may be higher, thus increasing the diimide yield. In the presence of coadsorbed oxygen, the yield of diimide decreases substantially. We propose that coadsorbed oxygen decreases the surface NH(ad) concentration, thus decreasing the yield of diimide formation.

In summary, diimide formation has been observed as a gas-phase product during hydrazine and ammonia decomposition on a clean Rh surface. Mass spectroscopy has been used to identify diimide. Diimide formation has been chemically confirmed since diimide yield increases substantially by coadsorption of hydrogen and decreases substantially by coadsorption of oxygen. Our results suggest that NH may be a stable surface intermediate during hydrazine and ammonia decomposition on Rh surface.

Strong Lewis Acids Derived from Molybdenum and Tungsten Nitrosyls Containing the Tri-2-pyridylmethane Ligand. Dynamic NMR Studies of Their Adducts with Aldehydes, Ketones, and Esters

J. W. Faller* and Yinong Ma

Contribution from the Department of Chemistry, Yale University, New Haven, Connecticut 06511.
Received June 27, 1990

Abstract: The doubly charged Lewis acid percursors $[HC(py)_3M(NO)_2(CO)](SbF_6)_2$ (M = Mo, W; $HC(py)_3$ = tri-2-pyridylmethane) are conveniently synthesized by reaction of $HC(py)_3M(CO)_3$ and 2 equiv of $NOSbF_6$. Facile loss of CO from the precursors generates the $[HC(py)_3M(NO)_2](SbF_6)_2$ Lewis acids. The Lewis acidity of the tungsten complex is greater than that of the molybdenum complex. With the ^1H NMR chemical shifts of bound crotonaldehyde as a qualitative assessment of relative acidity, the acidity of the tungsten species is comparable to that of BF_3 and $AlCl_3$, while that of the molybdenum species is similar to that of $TiCl_4$. Analysis of the NMR spectra of the Lewis acid–organic carbonyl base adducts, which include the adducts of aldehydes, ketones, and esters, showed that η^1-M(O=C) interactions dominate the chemistry. The barriers of rotation about the aldehyde C_1–C_2 bonds in the *p*-anisaldehyde adducts of the molybdenum and tungsten species were measured to be 12.8 and 13.7 kcal/mol, respectively, which are significantly higher than that for the free *p*-anisaldehyde. The exchange behavior between the *E* and *Z* isomers of the acetate adducts could be observed on the NMR time scale. The *E* to *Z* interconversion barriers of 12.2 ± 0.1 and 12.3 ± 0.1 kcal/mol for the methyl acetate and ethyl acetate complexes, respectively, were calculated from the results of variable-temperature proton NMR experiments. The free energy differences between the *E* and *Z* conformers of the methyl acetate and ethyl acetate adducts are 1.27 ± 0.01 and 0.96 ± 0.01 kcal/mol at 229 K, respectively.

Introduction

The complexation of organic carbonyl compounds with transition-metal complex Lewis acids can have a dramatic effect on the rates and selectivities of reactions at carbonyl centers, owing to the steric bulk and chirality of the ligands as well as to the electronic character of the metal centers.[1,2] An understanding of the structural and conformational aspects of the metal Lewis acid–carbonyl compound complexes should provide insight into reaction mechanisms, particularly with regard to selectivity. In the last decade, a number of transition-metal Lewis acid adducts of ketones and aldehydes have been isolated.[2,3] With a view to studying the interaction of transition-metal Lewis acids with carbonyl compounds, the reactions of $[HC(py)_3M(CO)(NO)_2](SbF_6)_2$ (M = Mo, W) with representative aldehydes, ketones, and acetate esters have been examined. NMR spectroscopic studies of various adducts have been undertaken, and the structural characteristics and chemical properties of these will be discussed here. The reaction of nitrosyl salts with low-valent transition-metal complexes have been widely used as a route to nitrosyl[4,5] complexes of both molybdenum and tungsten. Reaction of (tri-2-pyridylmethane)tricarbonylmolybdenum and -tungsten with nitrosyl hexafluoroantimonate forms highly charged cationic species $[HC(py)_3M(NO)_2(CO)](SbF_6)_2$. The high effective positive charge on the metal atom labilizes the π-acceptor ligand CO. This labilizing effect makes the $[HC(py)_3M(NO)_2(CO)](SbF_6)_2$ compounds excellent precursors for the facile generation of $[HC(py)_3M(NO)_2]^{2+}$ Lewis acids.

Experimental Section

Solvents were dried with use of standard procedures, and all manipulations were performed with Schlenk techniques unless specified otherwise. Proton NMR spectra were recorded at 250 and 500 MHz with Bruker spectrometers, and chemical shifts are reported (ppm) downfield from tetramethylsilane, with the solvent resonances for calibration. Temperatures were calibrated with the empirical correlation developed by Van Geet.[6] Nitromethane-d_3 was stored over molecular sieves under

(1) Sato, S.; Matsuda, I.; Izumi, Y. *Tetrahedron Lett.* **1986**, *27*, 5517.
(2) η^2-Ketone and aldehyde complexes: (a) Fernández, J. M.; Emerson, K.; Larsen, R. H.; Gladysz, J. A. *J. Am. Chem. Soc.* **1986**, *108*, 8268 and references therein. (b) Harman, W. D.; Fairlie, D. P.; Taube, H. *J. Am. Chem. Soc.* **1986**, *108*, 8223 and references therein. (c) Countryman, R.; Penfold, B. R. *Chem. Commun.* **1971**, 1598. (d) Kropp, K.; Skibbe, V.; Erker, G.; Krüger, C. *J. Am. Chem. Soc.* **1983**, *105*, 3353. (e) Brunner, H.; Wachter, J.; Bernal, I.; Creswick, M. *Angew. Chem., Int. Ed. Engl.* **1979**, *18*, 861. (f) Kaiser, J.; Sieler, J.; Walther, D.; Dinjus, E.; Golic, L. *Acta Crystallogr.* **1982**, *B39*, 1584.
(3) η^1-Ketone and aldehyde complexes: (a) Silverthorn, W. E. *Chem. Commun.* **1971**, 1310. (b) Williams, W. E.; Lalor, F. J. *J. Chem. Soc., Dalton Trans.* **1973**, 1329. (c) Foxman, B. M.; Klemarczyk, R. T.; Liptrot, R. E.; Rosenblum, M. *J. Organomet. Chem.* **1980**, *187*, 253. (d) Schmidt, E. K. G.; Thiel, C. H. *J. Organomet. Chem.* **1981**, *209*, 373. (e) Boudjouk, P.; Woell, J. B.; Radonovich, L. J.; Eyring, M. W. *Organometallics* **1982**, *1*, 582. (f) Bennett, M. A.; Matheson, T. W.; Robertson, G. B.; Steffen, W. L.; Turney, T. W. *Chem. Commun.* **1979**, 32. (g) Huang, Y.-H.; Gladysz, J. A. *J. Chem. Educ.* **1988**, *65*, 298.
(4) (a) Green, M.; Taylor, S. H. *J. Chem. Soc., Dalton Trans.* **1972**, 2629. (b) Sen, A.; Thomas, R. *Organometallics* **1982**, *1*, 1251.
(5) Stewart, R. P., Jr.; Moore, G. T. *Inorg. Chem.* **1975**, *14*, 2699.
(6) Van Geet, A. L. *Anal. Chem.* **1970**, *42*, 679.

0002-7863/91/1513-1579$02.50/0

nitrogen. Infrared spectra were obtained with a Nicolet 5SX-FTIR spectrophotometer. Elemental analyses were performed by Atlantic Microlab, Atlanta, GA. NMR samples of the Lewis acid–base adducts were all prepared in situ with an excess of organic base in each case. When an NMR sample of a pure adduct was desired, the excess organic substrate could be eliminated by carefully concentrating the sample mixture under vacuum and washing the resulting residues with methylene chloride.

Ligand Synthesis. Tri-2-pyridylmethanol was prepared by the method of Wilbaut and co-workers[7] from 2-lithiopyridine and recrystallized 2,2'-dipyridyl ketone. The $HOC(py)_3$ was obtained in 61% yield as white crystals from acetone; mp 127–128 °C (lit.[7] mp 127–128 °C).

Tri-2-pyridylchloromethane was prepared by a modification of the procedure of White and Faller.[8] Tri-2-pyridylmethanol (15.0 g, 0.057 mol) in 400 mL of THF was added dropwise to 1.7 g (0.071 mol) of a NaH suspension in 100 mL of THF. The resulting beige solution was treated dropwise with a solution of 8.5 g of thionyl chloride (0.071 mol) in 60 mL of THF over 30 min. An additional 2 h of stirring was allowed before the reaction was quenched with 200 mL of saturated $NaHCO_3$ solution. The residue from the organic layer after solvent removal was combined with the methylene chloride extracts of the aqueous layer. This solution was washed successively with 1 N $NaHCO_3$ and saturated NaCl solution and dried over sodium sulfate to give a beige crystalline solid after removal of solvent on a rotary evaporator. An acetone solution of the residue was decolorized with activated charcoal and filtered. Recrystallizations of the filtrate gave 14.4 g (90%) of white crystals, mp 165–166 °C (lit.[8] mp 166–167 °C).

Tri-2-pyridylmethane ($HC(py)_3$). To 17.5 g (0.0621 mol) of tri-2-pyridylchloromethane in 600 mL of THF under N_2 was added 45.0 mL (48.6 g, 0.167 mol) of n-Bu_3SnH via syringe. The resulting solution was heated to 45 °C, irradiated with ultraviolet light for 3 min, and allowed to stir at this temperature overnight. After the solution was cooled to room temperature, the solvent was partially removed on a rotary evaporator and the white precipitate was filtered and washed with 200 mL of pentane in three portions followed by 50 mL of diethyl ether. Recrystallizations of the crude white solid from acetone gave 14.1 g (92%) of white crystals, mp 98–99 °C (lit.[8] mp 99–100 °C).

Preparation of $HC(py)_3Mo(CO)_3$. A mixture of 1.0 g of tri-2-pyridylmethane (4.0 mmol) and 1.1 g (4.0 mmol) of $Mo(CO)_6$ suspended in 50 mL of acetonitrile was heated under reflux for 3 h under N_2 to give an orange precipitate. The precipitate was filtered and washed with CH_2Cl_2 to yield 1.6 g of $HC(py)_3Mo(CO)_3$ (92%). IR (KBr): $\nu_{C=O}$ 1897 (s), 1769 (br) cm^{-1}. Anal. Calcd for $C_{19}H_{13}N_3O_3Mo$: C, 53.41; H, 3.07; N, 9.83. Found: C, 53.31; H, 3.10; N, 9.79.

Preparation of $HC(py)_3W(CO)_3$. A suspension of 1.3 g of $W(CO)_6$ (3.7 mmol) in 100 mL of acetonitrile was heated under reflux under N_2. After 48 h, tri-2-pyridylmethane (0.82 g, 3.3 mmol) was added to the yellow solution. The mixture was heated to reflux for an additional 12 h, during which time a red precipitate formed. After the mixture was cooled, the supernatant was decanted and the red precipitate was washed with CH_2Cl_2 and dried in vacuo overnight to yield 1.70 g of $HC(py)_3W(CO)_3$ (99% based on $HCpy_3$ added). IR (KBr): $\nu_{C=O}$ 1885 (s), 1763 (br) cm^{-1}. Anal. Calcd for $C_{19}H_{13}N_3O_3W$: C, 44.30; H, 2.54; N, 8.16. Found: C, 44.39; H, 2.57; N, 7.97.

Preparation of $[HC(py)_3M(CO)(NO)_2](SbF_6)_2$. To a suspension of 96 mg of $HC(py)_3W(CO)_3$ in 5 mL of acetonitrile was added 2 equiv of $NOSbF_6$ (99 mg), and vigorous gas evolution immediately occurred. After it was stirred for 5 min, the resulting dark green solution was treated with 15 mL of methylene chloride to give a green precipitate. (Prolonged exposure of the compound to the solvent causes the solvent molecule to replace CO.) The precipitate was dried in vacuo overnight to yield 130 mg of $[HC(py)_3W(CO)(NO)_2](SbF_6)_2$ (76%). ^1H NMR (CD_3NO_2, 25 °C, 250 MHz): δ 7.79–9.19 (m, 12 H, $HC(py)_3$, 6.73 (s, 1 H, $HC(py)_3$). ^{13}C NMR (CD_3NO_2, 30 °C, 125 MHz): δ 192.7 (1 C, CO). IR (CH_3CN): $\nu_{C=O}$ 2145 (s); $\nu_{N=O}$ 1835 (s), 1753 (s) cm^{-1}. Anal. Calcd for $C_{17}H_{13}O_3N_5Sb_2F_{12}W$: C, 20.61; H, 1.32; N, 7.07. Found: C, 20.59; H, 1.36; N, 7.04.

$[HC(py)_3Mo(CO)(NO)_2](SbF_6)_2$ can be formed as a precipitate by adding 2 equiv of $NOSbF_6$ to a suspension of $HC(py)_3Mo(CO)_3$ in a 1:1 mixture of methylene chloride and nitromethane at 0 °C. Because of the extreme lability of the carbonyl ligand in this complex, no analytical measurements could be carried out without experiencing either the partial or complete loss of the carbonyl group. The compound was presumed to have a structure similar to that of the analogous tungsten complex as indicated by its IR. IR (Nujol): $\nu_{C=O}$ = 2159 (s); $\nu_{N=O}$ 1860 (s), 1796 (s) cm^{-1}. The reaction of $HC(py)_3Mo(CO)_3$ with 2 equiv of $NOBF_4$ and $NOSbF_6$ in acetonitrile only gave the solvent complexes $[HC(py)_3Mo(CH_3CN)(NO)_2](BF_4)_2$ and $[HC(py)_3Mo(CH_3CN)(NO)_2](SbF_6)_2$. The former was characterized. IR (CH_3CN): $\nu_{N=O}$ 1833 (s), 1734 (s) cm^{-1}. Anal. Calcd for $C_{18}H_{16}O_2N_6B_4F_8Mo$: C, 34.99; H, 2.61; N, 13.60. Found: C, 34.83; H, 2.63; N, 13.50.

$[HC(py)_3W(CH_3CN)(NO)_2](SbF_6)_2$ was obtained by stirring $[HC(py)_3W(CO)(NO)_2](SbF_6)_2$ in acetonitrile overnight. ^1H NMR (CD_3NO_2, 25 °C, 250 MHz): δ 7.72–9.98 (m, 12 H, $HC(py)_3$), 6.67 (s, 1 H, $HC(py)_3$), 2.68 (s, 3 H, CH_3CN). IR (CH_3CN): $\nu_{N=O}$ 1800 (s), 1709 (s) cm^{-1}. Anal. Calcd for $C_{18}H_{16}O_2N_6Sb_2F_{12}W$: C, 21.54; H, 1.61; N, 8.37. Found: C, 21.65; H, 1.66; N, 8.35.

NMR Studies of Reactions of $[HC(py)_3M(NO)_2(CO)](SbF_6)_2$ with Aldehydes, Ketones, and Acetates. (1) *trans*-Cinnamaldehyde. A solution of $[HC(py)_3W(NO)_2(CO)](SbF_6)_2$ in CD_3NO_2 with a slight excess of *trans*-cinnamaldehyde was sealed in an NMR sample tube and then heated at 80 °C for about 30 min until no starting material resonances were observed in the ^1H NMR spectrum. This was achieved by monitoring pyridyl ortho-proton resonances for which the differences in chemical shifts between the starting material and adduct are very significant. ^1H NMR (CD_3NO_2, 25 °C, 250 MHz): δ 6.73 (s, 1 H, $HC(py)_3$), 10.09 (d, 1 H, HC=O, $J_{H-H'}$ = 8.5 Hz, J_{W-H} = 3.3 Hz, $\Delta\delta$[9] = 0.44), 7.37 (dd, 1 H', CH'=CH'', $J_{H'-H''}$ = 15.3 Hz, $J_{H'-H}$ = 8.5 Hz, $\Delta\delta$ = 0.64), 8.59 (d, 1 H'', CH'=CH'', $J_{H'-H''}$ = 15.3 Hz, $\Delta\delta$ = 0.95), aromatic proton resonances are obscured. ^{13}C NMR (CD_3NO_2, 30 °C, 125 MHz, broad-band decoupling): δ 209.1 (s, 1 C, C=O). For the molybdenum species, no heating was necessary and the formation of the adduct was complete within 1 h. ^1H NMR (CD_3NO_2, 25 °C, 250 MHz): δ 6.68 (s, 1 H, $HC(py)_3$), 10.03 (d, 1 H, HC=O, $J_{H-H'}$ = 8.7 Hz, $\Delta\delta$ = 0.38), 7.32 (dd, 1 H', CH'=CH'', $J_{H'-H''}$ = 15.6 Hz, $J_{H'-H}$ = 8.7 Hz, $\Delta\delta$ = 0.59), 8.48 (d, 1 H'', CH'=CH'', $J_{H'-H''}$ = 15.6 Hz, $\Delta\delta$ = 0.84).

(2) α-Methyl-*trans*-cinnamaldehyde. The procedure was similar to that for the *trans*-cinnamaldehyde experiment. ^1H NMR for M = W (CD_3NO_2, 25 °C, 250 MHz): δ 6.72 (s, 1 H, $HC(py)_3$), 10.08 (s, 1 H, HC=O, $^3J_{W-H}$ < 2 Hz, $\Delta\delta$ = 0.58), the chemical shift of H_β is obscured by aromatic protons, 2.12 (s, 3 H, Me, $\Delta\delta$ = 0.10).

(3) Crotonaldehyde. The procedures were similar to those for the *trans*-cinnamaldehyde experiments. ^1H NMR for M = W (CD_3NO_2, 25 °C, 250 MHz): δ 6.72 (s, 1 H, $HC(py)_3$), 9.97 (d, 1 H, HC=O, $J_{H-H'}$ = 8.9 Hz, J_{W-H} = 3.5 Hz, $\Delta\delta$ = 0.56), 6.80 (m, 1 H_2, $\Delta\delta$ = 0.71), 8.20 (m, 1 H_3, $\Delta\delta$ = 1.19), 2.38 (m, 3 H, Me, $\Delta\delta$ = 0.36). ^{13}C NMR for M = W (CD_3NO_2, 30 °C, 125 MHz, broad-band decoupling): δ 211.1 (s, 1 C, C=O, $\Delta\delta$ = 15.9). For M = Mo, ^1H NMR (CD_3NO_2, 25 °C, 250 MHz): δ 6.47 (s, 1 H, $HC(py)_3$), 9.88 (d, 1 H, HC=O, $J_{H-H'}$ = 8.9 Hz, $\Delta\delta$ = 0.47), 6.73 (m, 1 H_2, $\Delta\delta$ = 0.66), 8.05 (m, 1 H_3, $\Delta\delta$ = 1.05), 2.36 (m, 3 H, Me, $\Delta\delta$ = 0.33).

(4) *p*-Anisaldehyde. The procedures were similar to those for the *trans*-cinnamaldehyde experiments. ^1H NMR for M = W (CD_3NO_2, 25 °C, 250 MHz): δ 6.73 (s, 1 H, $HC(py)_3$), 10.22) (s, 1 H, HC=O, $\Delta\delta$ = 0.40), 7.75–8.93 (m, 12 H, 3 py), 8.18 (br, 2 H, ortho protons), 7.20 (br 2 H, meta protons), 4.05 (3.92 for the free *p*-anisaldehyde) (s, 3 H, OMe). ^{13}C NMR for M = W (CD_3NO_2, 30 °C, 125 MHz, broad-band decoupling): δ 204.6 (s, 1 C, C=O, $\Delta\delta$ = 11.9). ^1H NMR for M = Mo (CD_3NO_2, 25 °C, 250 MHz): δ 6.73 (s, 1 H, $HC(py)_3$), 10.22 (s, 1 H, HC=O, $\Delta\delta$ = 0.40), 7.75–8.93 (m, 12 H, 3 py), 8.18 (br 2 H, ortho protons), 7.20 (br, 2 H, meta protons), 4.05 (s, 3 H, OMe, $\Delta\delta$ = 0.13).

(5) Benzaldehyde. The procedures were similar to those for the *trans*-cinnamaldehyde experiments. ^1H NMR for M = W (CD_3NO_2, 25 °C, 250 MHz): δ 6.76 (s, 1 H, $HC(py)_3$), 10.59 (s, 1 H, HC=O, $\Delta\delta$ = 0.63), aromatic proton chemical shifts are obscured. ^{13}C NMR for M = W (CD_3NO_2, 30 °C, 125 MHz, broad band decoupling): δ 210.8 (s, 1 C, C=O, $\Delta\delta$ = 16.0). ^1H NMR for M = Mo (CD_3NO_2 25 °C, 250 MHz): δ 6.70 (s, 1 H, $HC(py)_3$), 10.50 (s, 1 H, HC=O, $\Delta\delta$ = 0.54).

(6) Ferrocenecarboxaldehyde. The procedures were similar to those for the *trans*-cinnamaldehyde experiments. However, for the formation of the tungsten complex, heating at lower temperature, i.e., 65 °C, was sufficient to form the complex in the same period of time. ^1H NMR for M = W (CD_3NO_2, 25 °C, 250 MHz): δ 6.69 (s, 1 H, $HC(py)_3$), 8.99–7.81 (m, 12 H $HC(py)_3$), 10.32 (s, 1 H, HC=O, $\Delta\delta$ = 0.44), 5.62 (br t, 2 H, H_αCp, $\Delta\delta$ = 0.81), 5.03 (t, 2 H, H_βCp, $\Delta\delta$ = 0.36), 4.73 (s, 5 H, HCp, $\Delta\delta$ = 0.41). ^1H NMR for M = Mo (CD_3NO_2, 25 °C, 250 MHz): δ 6.66 (s, 1 H, $HC(py)_3$), 8.80–7.44 (m, 12 H, $HC(py)_3$), 10.32 (s, 1 H, HC=O, $\Delta\delta$ = 0.44), 5.48 (br t, 2 H, H_αCp, $\Delta\delta$ = 0.67), 5.03 (t, 2H, H_βCp, $\Delta\delta$ = 0.36), 4.64 (s, 5 H, HCp, $\Delta\delta$ = 0.32).

(7) Acetone. The procedures were similar to those for the *trans*-cinnamaldehyde experiments. ^1H NMR for M = W (CD_3NO_2, 25 °C, 250 MHz): δ 6.72 (s, 1 H, $HC(py)_3$), 2.93 (s, 6 H, $\Delta\delta$ = 0.83), 7.7–8.9 (m,

(7) Wilbaut, J. P.; De Jonge, A. P.; Van der Voort, H. G. P.; Otto, H. L. *Recl. Trav. Chim. Pays-Bas* **1951**, *70*, 1054.

(8) White, D. L.; Faller, J. W. *Inorg. Chem.* **1982**, *21*, 3119.

(9) Downfield shift (ppm) from the corresponding chemical shift of the uncoordinated compound.

12 H, 3 py). ^{13}C NMR for M = W (CD_3NO_2, 25 °C, 125 MHz, broad-band decoupling): δ 239.4 (1 C, C=O, Δδ = 28.0), 34.2 (2 C, 2 CH_3, Δδ = 3.3). ^1H NMR for M = Mo (CD_3NO_2, 25 °C, 250 MHz): δ 6.67 (s, 1 H, $HC(py)_3$), 2.89 (s, 6 H, 2 CH_3, Δδ = 0.79), 7.6–9.1 (m, 12 H, 3 py).

(8) 2-Cyclohexen-1-one. The procedures were similar to those for the *trans*-cinnamaldehyde experiments. ^1H NMR for M = W (CD_3NO_2, 25 °C, 250 MHz): δ 6.70 (s, 1 H, $HC(py)_3$), 7.75–8.91 (m, 12 H, 3 py), 7.64 (dt, 1 H_2, Δδ = 0.74), 8.13 (dt, 1 H_3, Δδ = 1.06), 2.79 (m, 2 H_4, Δδ = 0.45), 2.33 (m, 2 H_5, Δδ = 0.34), 3.13 (m, 2 H_6, 0.80). ^{13}C NMR for M = W (CD_3NO_2, 25 °C, 125 MHz, broad-band decoupling): δ 218.8 (1 C, C=O, Δδ = 17.7). ^1H NMR for M = Mo (CD_3NO_2, 25 °C, 250 MHz): δ 6.66 (s, 1 H, $HC(py)_3$), 7.70–8.80 (m, 12 H, 3 py), 7.60 (dt, 1 H_2, Δδ = 0.63), 8.02 (dt, 1 H_3, Δδ = 0.84), 2.76 (m, 2 H_4, Δδ = 0.42), 2.30 (m, 2 H_5, Δδ = 0.29), 3.10 (m, 2 H_6, Δδ = 0.71).

(9) Methyl Acetate. For M = W, only, the procedure was similar to that for the aldehyde experiment except for the longer duration of heating; the reaction takes 60 min at 80 °C to complete. At −44 °C, the limiting spectrum is observed having resonances due to each conformer (*Z*:*E*) in a relative ratio of 100:6.19. ^1H NMR (CD_3NO_2, −44 °C, 250 MHz): major (*Z* conformer) δ 6.73 (s, 1 H, $HC(py)_3$), 7.74–8.93 (m, 12 H, 3 py), 3.80 (s, 3 H, OCH_3), 2.91 (s, 3 H, CH_3C=O); minor (*E* conformer) δ 6.73 (s, 1 H, $HC(py)_3$), 7.75–8.94 (m, 12 H, 3 py), 4.58 (s, 3 H, OCH_3), 2.70 (s, 3 H, CH_3C=O).

(10) Ethyl Acetate. For M = W only, the procedure was similar to that for the methyl acetate experiment. ^1H NMR (CD_3NO_2, 47 °C, 250 MHz): δ 6.67 (s, 1 H, $HC(py)_3$), 7.76–8.89 (m, 12 H, 3 py), 4.37 (q, 2 H, OCH_2), 1.30 (t, 3 H, OCH_2CH_3), 2.88 (s, 3 H, CH_3C=O). At −44 °C, the limiting spectrum is observed having resonances for each conformer (*Z*:*E*) in a relative ratio of 100:12.1. ^1H NMR (CD_3NO_2, −44 °C, 250 MHz): major (*Z* conformer) δ 6.73 (s, 1 H, $HC(py)_3$), 7.75–8.93 (m, 12 H, 3 py), 4.18 (q, 2 H, OCH_2), 1.15 (t, 3 H, OCH_2CH_3), 2.89 (s, 3 H, CH_3C=O); minor (*E* conformer) δ 6.73 (s, 1 H, $HCpy_3$), 7.75–8.94 (m, 12 H, 3 py), 4.91 (q, 2 H, OCH_2), 1.64 (t, 3 H, OCH_2CH_3), 2.69 (s, 3 H, CH_3C=O).

(11) *tert*-Butyl Acetate. An excess of *tert*-butyl acetate was added to a solution of tungsten Lewis acid species $[HC(py)_3W(NO)_2](SbF_6)_2$ in CD_3NO_2, which was first generated by heating a solution of $[HC(py)_3W(NO)_2(CO)](SbF_6)_2$ in CD_3NO_2 at 80 °C for 1 h. An instant dissociation of *tert*-butyl acetate promoted by the Lewis acid occurred, and one of the decomposition products (isobutylene) underwent rapid catalytic oligomerization. The Lewis acid formed an adduct with the other decomposition product (acetic acid) whose proton NMR spectrum is described as follows. ^1H NMR (CD_3NO_2, 25 °C, 250 MHz): δ 6.67 (s, 1 H, $HC(py)_3$), 7.73–8.91 (m, 12 H, 3 py), 2.05 (s, 1 H, OH), 2.73 (s, 3 H, CH_3C=O, Δδ = 0.71).

Results and Discussion

Preparation of $[HC(py)_3M(NO)_2L](SbF_6)_2$. At ambient temperature, the treatment of $HC(py)_3Mo(CO)_3$ with 2 equiv or more of nitrosyl hexafluoroantimonate in either acetonitrile or acetone gave the corresponding green dinitrosyl solvent derivatives (eq 1). The corresponding carbonyl dinitrosyl complex could only be obtained when the reaction was carried out at temperatures below 0 °C in a 1:1 mixture of methylene chloride and nitromethane (eq 2). The infrared spectrum of a Nujol mull had a $\nu_{C=O}$ band

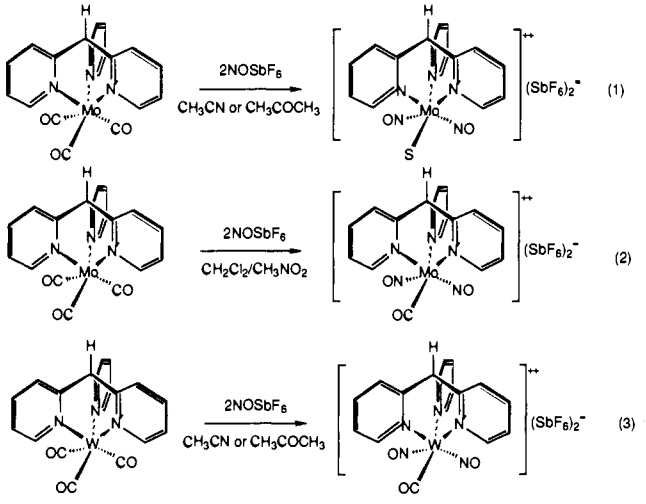

at an extraordinarily high frequency (2159 cm^{-1}), which is higher than the value for free CO[10] (2143 cm^{-1}) and the value of 2129 cm^{-1} for the analogous $[CpMo(NO)_2(CO)]PF_6$.[5] In addition to the carbonyl stretch, the two strong NO stretching bands are observed at 1796 and 1860 cm^{-1}, which are typical of cis dinitrosyl species.[5] The analogous tungsten complex $[HC(py)_3W(NO)_2(CO)](SbF_6)_2$ was obtained by reaction of $NOSbF_6$ and $HC(py)_3W(CO)_3$ in acetonitrile (see eq 3). It was more stable and could be stored in air at room temperature for months without noticeable decomposition. Its IR spectrum in acetonitrile displays two strong nitrosyl bands at 1753 and 1835 cm^{-1}. A broad band at 2145 cm^{-1} is assigned to the carbonyl stretch, which is much higher than that (2116 cm^{-1}) of the analogous $[CpW(NO)_2(CO)]^+$ species[5] apparently owing to the greater positive charge on the tungsten atom.

A characteristic feature of the $[HC(py)_3M(NO)_2(CO)](SbF_6)_2$ complexes is the extreme lability of the carbonyl group. The carbonyl group in $[HC(py)_3W(CO)(NO)_2](SbF_6)_2$ can be readily replaced by donor solvent molecules such as acetone or acetonitrile under ambient conditions. The replacement of the carbonyl by acetonitrile was monitored by infrared spectroscopy; the half-life of $[HC(py)_3W(CO)(NO)_2](SbF_6)_2$ in acetonitrile is 5 h at room temperature. Acetone reacts with $[HC(py)_3W(CO)(NO)_2](SbF_6)_2$ much more slowly than does acetonitrile. The half-life for CO displacement from $[HC(py)_3W(CO)(NO)_2](SbF_6)_2$ in acetone is about 1 day. The carbonyl group can also be removed from the solid compound by heating above 100 °C. However, repeated attempts always resulted in incomplete decarbonylation, and no pure sample of $[HC(py)_3W(NO)_2](SbF_6)_2$ could be isolated.

The release of CO creates the 16-e cation $[HC(py)_3W(NO)_2]^{2+}$. This gives rise to a question as to whether a stabilizing W–F interaction occurs between the counterion SbF_6^- and the tungsten center as suggested by Hersh's isolation of the complex $(PMe_2Ph)(CO)_3(NO)WFSbF_5$.[11] No asymmetric broadening of the infrared absorption of ν_{Sb-F} at 660 cm^{-1} was observed, as has been found for a structurally characterized SbF_6 coordination complex.[12] A subsequent ^{19}F NMR study of $[HC(py)_3W(NO)_2](SbF_6)_2$ showed that both SbF_6^- ions were equivalent at room temperature, suggesting retention of octahedral symmetry or rapid exchange. These observations rule out the possibility of a strong nonlabile W–F interaction. A similar weak interaction was observed in $CpCr(NO)_2FPF_5$ by Regina and Wojcicki.[13a] Therefore, this $HC(py)_3$ complex can be used as a metal Lewis acid, in a manner similar to that demonstrated by the closely related Cp analogues derived from $CpM(NO)_2X$.[5,13]

Reactions of $[HC(py)_3M(NO)_2(CO)](SbF_6)_2$ with Aldehydes, Ketones, and Esters. The acetone complexes $[HC(py)_3M(NO)_2(Me_2C=O)](SbF_6)_2$ were prepared by stirring $[HC(py)_3M(NO)_2(CO)](SbF_6)_2$ in dry acetone. The ^1H NMR spectra show that the acetone methyl resonance has downfield shifts of 0.83 and 0.79 ppm relative to those of the uncoordinated acetone for the W and Mo complexes, respectively. The carbonyl carbon also has a downfield shift of 28 ppm in the ^{13}C NMR for the W complex. The NMR data are consistent with an η^1-acetone interaction. The observation of the same chemical shift for the nonequivalent methyls, as observed also for other η^1-acetone complexes,[3a,b,g] requires a rapid syn–anti interconversion on the NMR time scale at ambient temperature as previously suggested by Foxman et al.[3c] Intermolecular exchange between coordinated and uncoordinated acetone is not responsible for the syn–anti interconversion, since both the free and coordinated acetone resonances were observed as separate sharp resonances upon addition of acetone to the NMR sample, which indicates that this process is slow. Gladysz has proposed one possible mechanism in which the methyl groups exchange by an $\eta^1 \rightleftarrows \eta^2 \rightleftarrows \eta^1$ acetone

(10) Cotton, F. A.; Wilkinson, G. *Advanced Inorganic Chemistry*, 4th ed., Interscience: New York, 1980; p 85.
(11) Hersh, W. H. *J. Am. Chem. Soc.* **1985**, *107*, 4599.
(12) Shelly, K.; Barczak, T.; Sheidt, W. R.; Reed, C. A. *Inorg. Chem.* **1985**, *24*, 4325.
(13) (a) Regina, F. J.; Wojcicki, A. *Inorg. Chem.* **1980**, *19*, 3803. (b) Legzdins, P.; Martin, D. T. *Organometallics* **1983**, *2*, 1785.

Scheme I

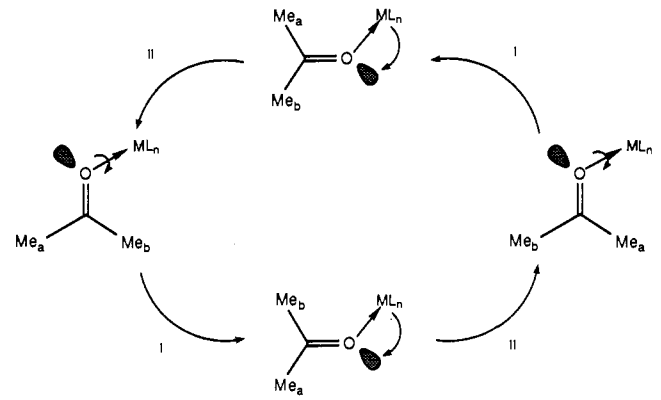

Table I. Aldehydic Proton Chemical Shifts of $[HC(py)_3W(NO)_2(\eta^1\text{-aldehyde})](SbF_6)_2$ Complexes in CD_3NO_2

complex	δ (ppm)	$\Delta\delta$ (ppm)[a]	J_{W-H} (Hz)
PhCHO	10.59 (s)	0.63	<2.0
p-CH_3OPhCHO	10.22 (s)	0.40	<2.0
trans-PhCH=CHCHO	10.03 (d)	0.38	3.3
trans-PhCH=C(Me)CHO	10.08 (s)	0.58	<2.0
trans-CH_3CH=CHCHO	9.88 (d)	0.47	3.5
FcCHO	10.32 (s)	0.44	<2.0

[a] Downfield shift from that of the corresponding uncoordinated aldehyde.

Table II. Aldehyde and Ketone Carbonyl ^{13}C Chemical Shifts of the $[HC(py)_3W(NO)_2]^{2+}$ Complexes in CD_3NO_2

complex	δ (ppm)	$\Delta\delta$ (ppm)[a]
CH_3COCH_3	239.4	28.0
PhCHO	210.8	16.0
p-CH_3OPhCHO	204.6	11.9
trans-CH_3CH=CHCHO	211.1	15.9
trans-PhCH=CHCHO	209.1	13.4
cyclohexenone	218.8	17.7

[a] Downfield shift from that of the corresponding uncoordinated aldehyde or ketone.

ligand isomerization.[3g] We, however, favor an alternative explanation in which no η^2 transition state is required. It is illustrated in Scheme I and consists of two steps: rotation of acetone about the donor–acceptor bond (step I) and migration to the other lone pair on the donor oxygen (step II). Barriers for the migration in BF_3 adducts of bulkier ketones have been estimated by ^{13}C NMR experiments to be 8–10 kcal/mol.[14] Of the two processes, the rotation about the M–O bond should have a much lower barrier; e.g., the activation barrier for rotation has been estimated at 1–2 kcal/mol for the case of the BF_3 adduct.[15]

The formation of an aldehyde adduct with the $HC(py)_3$ molybdenum Lewis acid can be readily accomplished by adding excess aldehyde to a solution of the Lewis acid precursor $[HC(py)_3Mo(NO)_2(CO)](SbF_6)_2$ in CD_3NO_2 and monitoring the reaction by ^1H NMR. The $[HC(py)_3W(NO)_2(\eta^1\text{-aldehyde})](SbF_6)_2$ complexes were obtained upon heating $[HC(py)_3W(NO)_2(CO)](SbF_6)_2$ in CD_3NO_2 with excess aldehyde (benzaldehyde, *p*-anisaldehyde, *trans*-cinnamaldehyde, and crotonaldehyde) at 80–90 °C for 30–40 min. The ^1H NMR and ^{13}C NMR spectral features of these aldehyde complexes are consistent with η^1-M—(O=C) interactions, which typically exhibit ^{13}C shifts within 20–30 ppm of their uncoordinated values.[16] The data for the tungsten adducts are summarized in Tables I and II. From the point of view of both steric and electronic considerations, it is very unlikely that the $[HC(py)_3M(NO)_2]^{2+}$ moieties form η^2

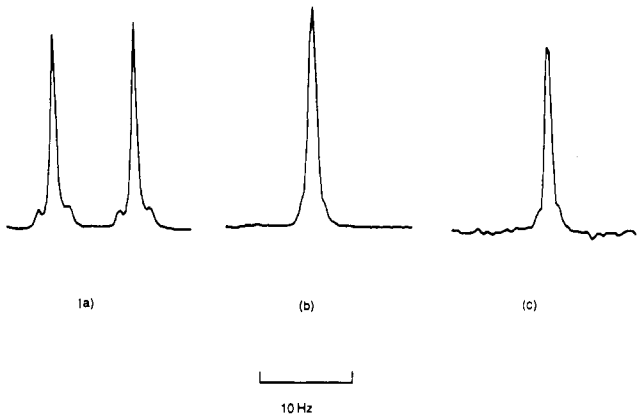

Figure 1. Aldehydic proton resonances of the tungsten adducts of (a) *trans*-cinnamaldehyde, (b) *p*-anisaldehyde, and (c) benzaldehyde.

adducts with carbonyl compounds. Firstly, the tri-2-pyridylmethane ligand is very bulky and, in turn, should not favor the sterically more demanding η^2 bonding. Secondly, the high charge on the cationic Lewis acid metal centers assures low metal π basicity, which does not favor η^2 bonding.

$^3J_{W-H}$ and Configurational Equilibria in the Aldehyde Adducts. Unusually large differences in coupling constants between ^{183}W and the aldehyde protons were noted. In the *trans*-cinnamaldehyde and crotonaldehyde complexes, $^3J_{W-H}$ of 3.3 and 3.5 Hz were observed, respectively. Apparently because of the much smaller $^3J_{W-H}$ (<2 Hz), no ^{183}W satellites were detected for the aldehydic protons in the *p*-anisaldehyde and benzaldehyde complexes (see Figure 1). These variations in average coupling constant appear to arise from different syn to anti isomer ratios in the various complexes. The syn and anti configurations should be characterized by very different $^3J_{W-H}$ coupling constants. Note that the syn isomers have the aldehydic proton trans to W while the anti isomers have the aldehydic proton cis to W. A significant difference in coupling constants between the syn (with trans W–H) and anti (with cis W–H) isomers would be expected by analogy to the difference between trans and cis proton coupling constants in the case of olefins.[18] Furthermore, in an NMR study of the protonated aldehydes the observed coupling constants between the acidic protons and the aldehydic hydrogens were very different in the anti isomers and in the syn isomers.[19] Because of the rapid interconversion between the syn and anti configurations, the observed $^3J_{W-H}$ of a tungsten adduct is the average coupling constant of the syn and anti isomers. For the *trans*-cinnamaldehyde and crotonaldehyde complexes, greater syn to anti ratios than those for the aryl aldehydes have resulted in larger average values of $^3J_{W-H}$ due to the greater contribution of trans $^3J_{W-H}$.

Although crystal structures of η^1-aldehyde complexes[17] would suggest that anti configurations should generally be more stable and predominate in solution equilibria, the relative populations of syn isomers could be higher for some adducts. The larger syn to anti ratios in cinnamaldehyde and crotonaldehyde adducts can be explained on the basis of steric considerations. The relative importance of these steric interactions can be seen in Figure 2 in which I represents an aryl aldehyde adduct and II represents an adduct of a trans α,β-unsaturated aldehyde. The significant differences in steric interactions occur in the syn isomers. Configuration Ib for an aryl aldehyde is more sterically congested than that for an α,β-unsaturated aldehyde in an s-trans conformation IIb′. Thus, the relative populations of the syn isomers in the cinnamaldehyde and crotonaldehyde complexes should be higher than those of the benzaldehyde and *p*-anisaldehyde adducts.

(14) Hartman, J. S.; Forsēn, S. *Tetrahedron Lett.* **1975**, 3497.
(15) LePage, T. J.; Wiberg, K. B. *J. Am. Chem. Soc.* **1988**, *110*, 6642.
(16) (a) Brown, J. M.; Chaloner, P. A. *J. Chem. Soc., Perkin Trans.* **1982**, *2*, 711. (b) Courtot, P.; Pichon, R.; Salaun, J. Y. *J. Organomet. Chem.* **1985**, *286*, C17. (b) Auffret, J.; Courtot, P.; Pichon, R.; Salaun, J. Y. *J. Chem. Soc., Dalton Trans.* **1987**, 1687.
(17) (a) Honeychuck, R. V.; Bonnesen, P. V.; Farahi, J.; Hersh, W. H. *J. Org. Chem.* **1987**, *52*, 5293. (b) Faller, J. W. Unpublished results on the crystal structures of $[CpFe(CO)_2(\text{benzaldehyde})]SbF_6$ and $[CpRu(CO)(PPh_3)(\eta^1\text{-}trans\text{-cinnamaldehyde})]SbF_6$.
(18) Sternhell, S. *Rev. Pure Appl. Chem.* **1964**, *15*, 14.
(19) (a) Brookhart, M.; Levy, G. C.; Winstein, S. *J. Am. Chem. Soc.* **1967**, *89*, 1735. (b) Olah, G. A.; Calin, M.; O'Brien, D. H. *J. Am. Chem. Soc.* **1967**, *89*, 3586.

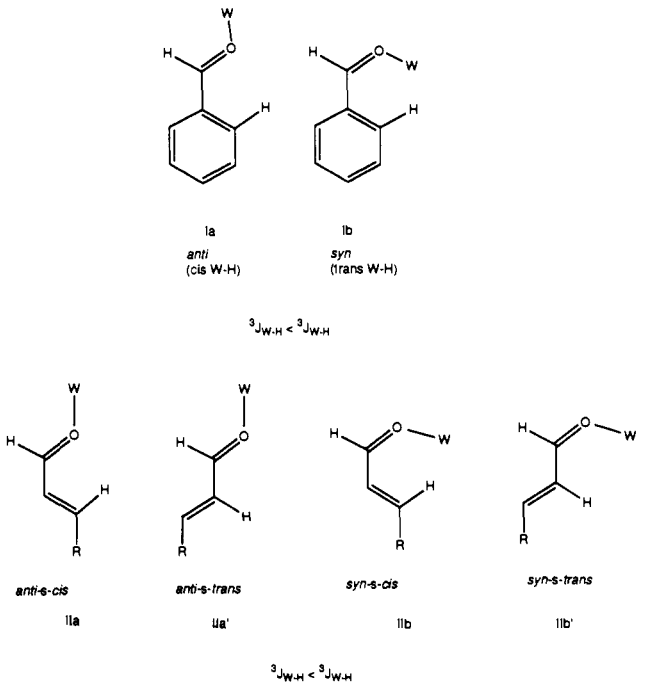

Figure 2. Conformational isomers of η^1-coordinated aldehydes.

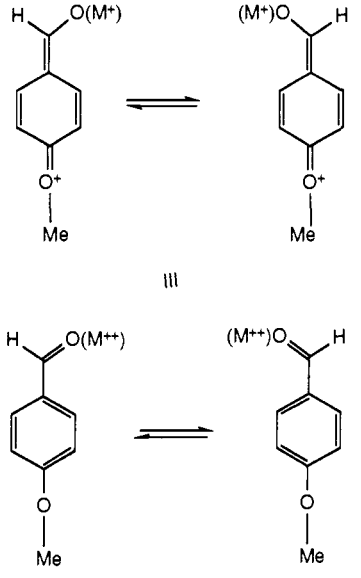

Figure 3. Resonance in a coordinated *p*-anisaldehyde.

Because of the increased interaction of the β-hydrogen with the Lewis acid, the s-cis conformation in the syn isomer should be destabilized relative to that in the anti isomer (i.e., [IIa]:[IIa'] > [IIb]:[IIb']). An increase in s-trans:s-cis ratio is consistent with the 0.9-Hz increase in the observed average $J(H_\alpha-H_{CHO})$ upon binding, although the electronic effect of binding also affects this quantity. Regardless, the availability of the sterically uncongested IIb' configuration allows for a significant syn isomer population in the α,β-unsaturated aldehydes and concomitant increased $^3J_{W-H}$. According to this argument, placing a methyl substituent at the α position in *trans*-cinnamaldehyde would increase the steric interactions in the syn configuration (particularly that in IIb') and, therefore, decrease the syn to anti ratio of the adduct. Indeed, in agreement with the expectations based on these steric considerations the (α-methyl-*trans*-cinnamaldehyde)tungsten complex showed no detectable ^{183}W satellites, i.e., $^3J_{W-H} < 2$ Hz.

Conformational Equilibria in Coordinated Aldehydes and Esters. Complexation by the $[HC(py)_3M(NO)_2]^{2+}$ Lewis acid produces a significant increase in the carboxaldehyde–phenyl C–C rotational barrier in the case of *p*-anisaldehyde complexes. The ^1H NMR spectra of the *p*-anisaldehyde complexes in nitromethane-d_3 show

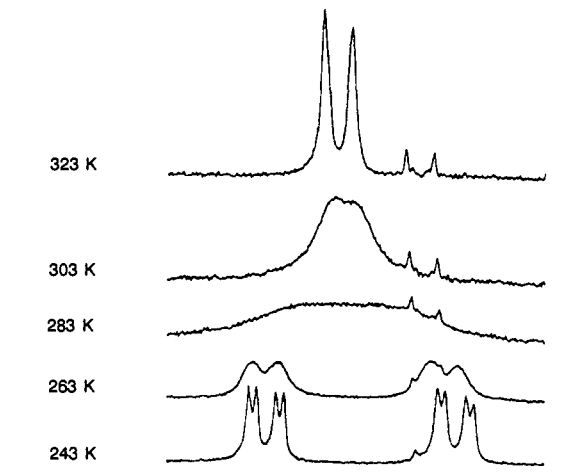

Figure 4. Variable-temperature ^1H NMR (CD_3NO_2, 250 MHz) of the two aromatic protons ortho to the methoxy group of $[HC(py)_3W(NO)_2(\eta^1\text{-}p\text{-anisaldehyde})](SbF_6)_2$. The two minor resonances are the corresponding protons of free *p*-anisaldehyde.

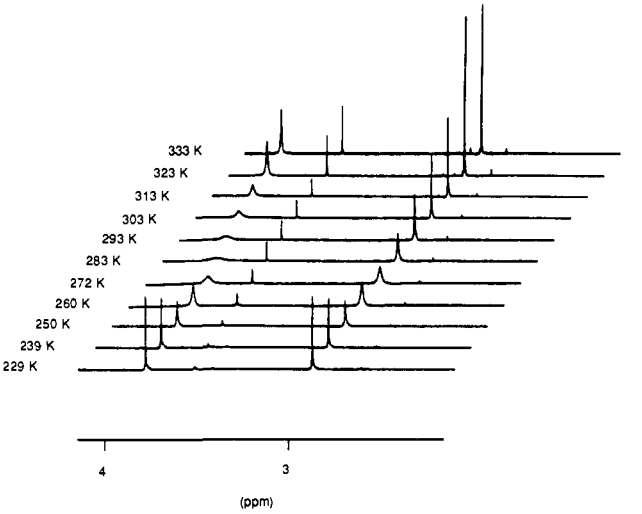

Figure 5. Variable-temperature ^1H NMR (CD_3NO_2, 250 MHz) of $[HC(py)_3W(NO)_2(\eta^1\text{-methyl acetate})](SbF_6)_2$.

two broad resonances that correspond to the two sets of averaging aromatic protons of the *p*-anisaldehyde group. This increase in the C–C rotational barrier may be rationalized by postulating an enhanced contribution of the ionic resonance structure (III in Figure 3), which is favored by the complexation. On the basis of the variable-temperature ^1H NMR data (Figure 4), the barriers are 13.7 and 12.8 kcal/mol[20] for the tungsten and molybdenum complexes, respectively, and are significantly higher than that for the uncoordinated *p*-anisaldehyde, which is 9.2 kcal/mol.[21] The rotational barrier for the tungsten adduct is comparable to the 14.2 kcal/mol observed for the *p*-anisaldehyde–BF_3 adduct.[22]

Other carbonyl bases, such as esters, also form stable complexes with the Lewis acid $[HC(py)_3W(NO)_2]^{2+}$. In contrast to the $[CpFe(CO)_2(CH_3COOCH_3)]^+$ adduct[3c] in which the ester is rapidly displaced by nitromethane, the extraordinarily strong donor–acceptor bond in ester complexes of $[HC(py)_3W(NO)_2(CH_3COOR)]^{2+}$ (R = CH_3, CH_2CH_3) makes it possible to generate them from the $[HC(py)_3W(NO)_2(CO)]^{2+}$ species and the corresponding ester by heating in nitronmethane solution. Complexation of acetates by the Lewis acids not only induces downfield shifts of the acetate resonances, as expected for binding

(20) The values of $\Delta G^\ddagger_{rot}$ were calculated at the coalescence temperatures (283, 263 K), according to the Eyring equation: $k_c = (kT/h)\exp(-\Delta G^\ddagger/RT)$, where $k_c = \pi(\nu_a - \nu_b)/2^{1/2}$.

(21) (a) Anet, F. A. L.; Ahmad, M. *J. Am. Chem. Soc.* **1964**, *86*, 119. (b) Klinck, R. E.; Marr, D. H. Stothers, J. B. *Chem. Commun.* **1967**, 409.

(22) Greenvald, A.; Rabinovitz, M. *Chem. Commun.* **1969**, 642.

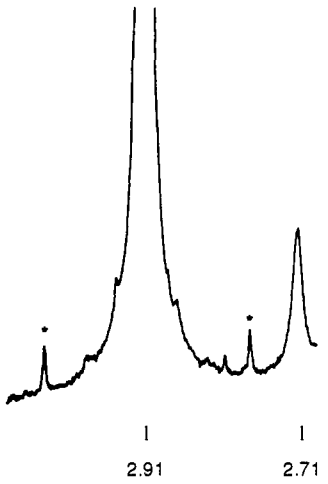

Figure 6. Acetyl methyl region of the ^{1}H NMR (CD_3NO_2, 250 MHz) of $[HC(py)_3W(NO)_2(\eta^1$-methyl acetate)$](SbF_6)_2$ at 229 K. ^{13}C satellites are indicated by an asterisk.

to a positive ion, but also produces conformational changes in the complexed acetates. This change in conformational equilibria is revealed by the line-shape variations of the complexed acetate proton resonances in the ^{1}H NMR variable-temperature spectra (see Figure 5), while the corresponding resonances of the free acetates do not show changes in the same temperature range. They do, however, broaden at lower temperatures (vide infra). The observed line-shape variations can be attributed to increased barriers of Z–E interconversion of the complexed acetates, analogous to that found for the p-anisaldehyde adduct, to reduced Z–E conformational energy differences compared with those of the corresponding free esters, or most likely to a combination of both effects. To the best of our knowledge, experimentally determined barrier heights for methyl acetate and ethyl acetate are not available. The barrier height for the Z–E interconversion of methyl acetate has been estimated to be 10–15 kcal/mol, and the free energy difference between E and Z conformers was reported as $\sim 8.5 \pm 1$ kcal/mol.[23] Variable-temperature ^{1}H NMR experiments were carried out in an attempt to measure the rotational barriers and equilibrium constants for the Z and E conformations of the complexed acetates. For both the methyl acetate and ethyl acetate complexes, minor conformers were observed at a limiting low temperature of 229 K with population ratios of 100:6.2 and 100:12, respectively (see Figures 6 and 7). An extensive investigation of the conformational isomerism in esters has demonstrated that the major conformer has a planar Z configuration;[24] hence, the major conformers here are tentatively assigned the Z configuration. Assuming that the relative stability of Z and E conformers has not been reversed by the complexation, values of ΔG for the equilibria in eqs 4 and 5 were calculated to be 1.27

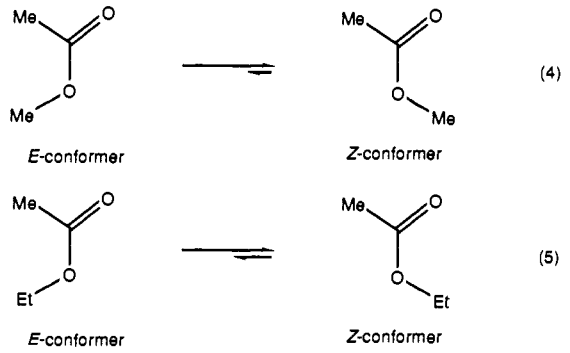

$\pm$ 0.01 and 0.96 $\pm$ 0.01 kcal/mol (229 K), respectively. Barriers

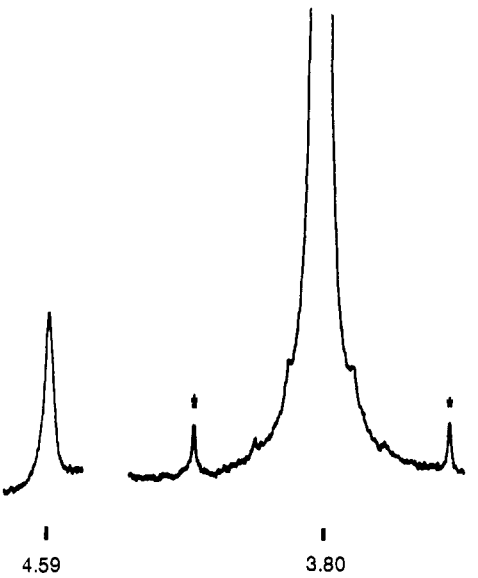

Figure 7. Methoxy methyl region of the ^{1}H NMR (CD_3NO_2, 250 MHz) of $[HC(py)_3W(NO)_2(\eta^1$-methyl acetate)$](SbF_6)_2$ at 229 K. ^{13}C satellites are indicated by an asterisk.

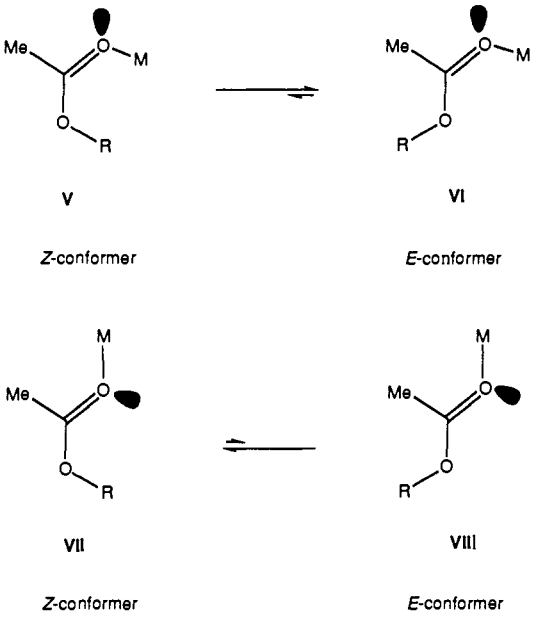

Figure 8. Z and E conformers of a coordinated acetate ester.

for conversion of the Z to the E conformer at 229 K ($\Delta G^{\ddagger}$) were obtained by line-shape analysis[25] and were found to be 13.2 $\pm$ 0.1 kcal/mol for the methyl acetate complex and 13.5 $\pm$ 0.1 kcal/mol for the ethyl acetate complex.

The larger E–Z free energy difference in methyl acetate compared with ethyl acetate is in accord with the trend observed for formates.[26] A considerable decrease in the E–Z energy difference between free and complexed methyl acetate ($\gg$3 vs 1.3 kcal/mol) was noted. This observation suggests that the complexation enhances the population of the E conformation, which is quite reasonable on the basis of steric considerations. As seen in the acetone complex, the metal center migrates rapidly between the two lone pairs on the acyl oxygen of acetate. When the metal center is trans to the acyl methyl, as shown in Figure 8, the Z conformation V is much more sterically demanding than the E conformation VI, owing to the repulsion between the methyl group

(23) Blom, C. E.; Günthard, H. H. *Chem. Phys. Lett.* **1981**, *84*, 267.
(24) For reviews, see: (a) Exner, O. In *The Chemistry of Double-Bonded Functional Groups*; Patai, S., Ed.; Interscience: London, 1977; p 1. (b) Jones, G. I. L.; Owen, N. L. *J. Mol. Struct.* **1973**, *18*, 1.
(25) The rate was determined with the formula $k = \pi W$, where W is the initial broadening in excess of the natural line width, and the Eyring equation: Faller, J. W. *Adv. Organomet. Chem.* **1977**, *16*, 211.
(26) Grindley, T. B. *Tetrahedron Lett.* **1982**, *23*, 1757.

Scheme II

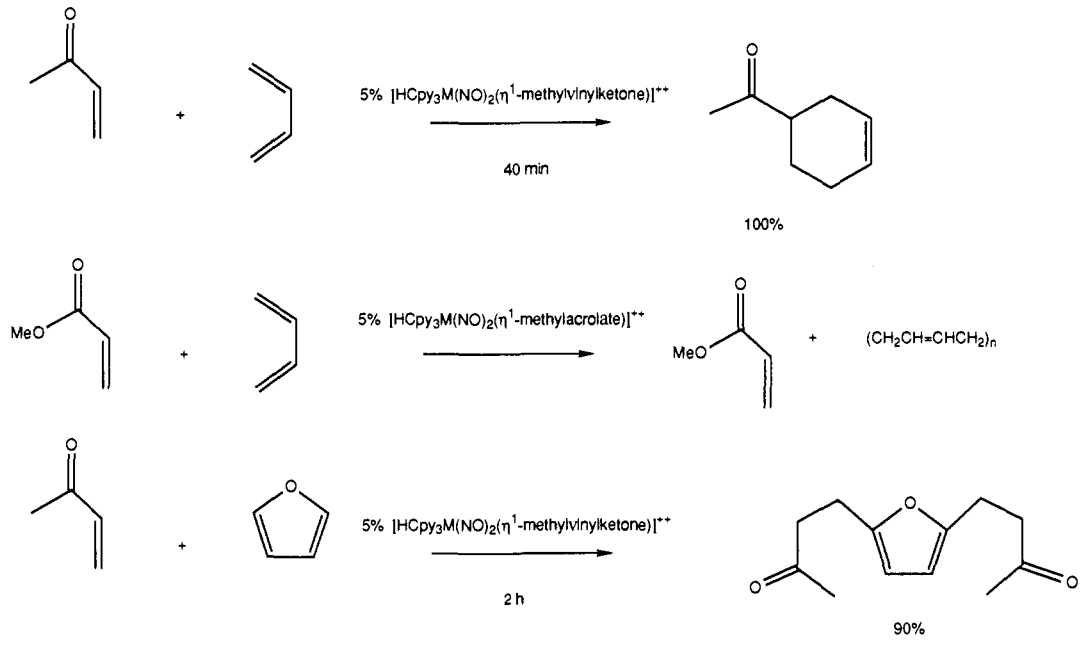

of the methoxy and the Lewis acid moiety. Since the metal would not be expected to have as great an effect on the analogous anti isomers VII and VIII, there must be a significant syn preference for the metal in order for the final *E*-conformer population to increase as much as it does.

The reaction between $[HC(py)_3W(NO)_2]^{2+}$ and *tert*-butyl acetate did not yield the corresponding adduct but led to decomposition of the ester. An oily mixture of isobutylene oligomers formed on the surface of the sample, and the NMR spectrum of the reaction mixture showed that an acetic acid adduct had formed. The oligomerization of isobutylene has also been observed to be catalyzed by the analogous Lewis acid $[CpW(NO)_2]^+$.[27]

Lewis Acidity of the Complexes and Lewis Basicity of Carbonyl Compounds. As seen clearly from the discussions above, $[HC(py)_3M(NO)_2](SbF_6)_2$ (M = Mo, W) complexes are very strong Lewis acids and form stable adducts with a variety of Lewis base organic carbonyl compounds. It would be interesting to compare their relative acidities with those of other metal complex Lewis acids, organometallic Lewis acids, and conventional Lewis acids. A number of methods have been developed with use of NMR chemical shift differences between free and Lewis acid complexed bases to scale the relative acidity of Lewis acids.[28] In a recent study of some organometallic Lewis acids by Hersh et al.,[29] the method developed by Childs[28a] was used in which coordination of crotonaldehyde gives a downfield shift of the 3-hydrogen in the ^1H NMR. For comparison, we have employed the same scale and the values are listed in Table III along with other published data. On the basis of this method, the acidity of the tungsten species is between those of $AlCl_3$ and BF_3, whereas that of the molybdenum species is comparable to that of $TiCl_4$. The fact that the tungsten species $[HC(py)_3W(NO)_2](SbF_6)_2$ is a stronger Lewis acid than the molybdenum analogue seems to be consistent with the results obtained in the study of the *p*-anisaldehyde adducts in which the activation barrier for rotation of the C–C bond (vide supra) in the tungsten adduct was measured to be 0.9 kcal/mol higher than that of the molybdenum adduct as a result of stronger donor–acceptor interaction. Normally, the acidity of congeners of transition metal would be expected to fall with increasing atomic volume, owing to the relatively weaker attraction between nuclear charge and incoming electron pairs.[30] Caution must be exercised, however, in discussing the relative acidity of second- and third-row transition metals based on this argument. Firstly, the trend is somewhat diminished by the influence of the lanthanide contraction and, secondly, a transition-metal acid with d electrons also may act as a "π-Lewis base" by participating in back-bonding with the LUMO of the Lewis base. This back-bonding effect may also increase along with atomic number within the same column. This may rationalize why a third-row metal complex can be a stronger Lewis acid than its second-row congener. However, the relative acidity of the W and Mo acids could be inverted by choosing Lewis bases with different "π-Lewis acid" abilities. Thus, caution should be used in assessing an overall Lewis acid strength with use of one specific base as a standard. The validity of using spectral parameters, such as the ^1H NMR shift of crotonaldehyde, for assessment of acidity may also be argued; nevertheless, these methods provide a useful basis for comparison and prediction of reactivity.

The relative basicity of organic carbonyl compounds toward these acids was evaluated by measuring equilibrium constants in competition experiments in which the relative concentrations of carbonyl complexes and pairs of free carbonyl-containing ligands were determined by integration of ^1H NMR resonances. The sequence of relative basicity measured in conjunction with the use of the tungsten Lewis acid $[HC(py)_3W(NO)_2](SbF_6)_2$ was as follows: 2-cyclohexen-1-one > *p*-anisaldehyde > *trans*-cinnamaldehyde > crotonaldehyde > acetone > ethyl acetate > benzaldehyde $\approx$ methyl acetate.

Reactivity. The strong activation of carbonyl species upon binding to the dinitrosyl species prompted us to examine their potential for catalytic activity in organic transformations. Some preliminary results are summarized in Scheme II. In the catalysis of the Diels–Alder reaction between methyl vinyl ketone and 1,3-butadiene, the [methyl vinyl ketone]–$[HC(py)_3W(NO)_2]$ adduct was generated by heating the carbonyldinitrosyl precursor at 70 °C for 30 min in CD_3NO_2 with excess dienophile (20 equiv) before the addition of butadiene (20 equiv). The Diels–Alder reaction was monitored by ^1H NMR. The half-life of this reaction is about 10 min at room temperature. The product was verified by comparison of its NMR spectrum with that of an authentic sample. On the other hand, the $[HC(py)_3M(NO)_2]^{2+}$ acids are also active butadiene polymerization catalysts. When a less basic

(27) Legzdins, P.; Richter-Addo, G. B.; Einstein, W. B.; Jones, R. H. *Organometallics* **1990**, *9*, 431.

(28) (a) Childs, R. F.; Mulholland, D. L.; Nixon, A. *Can. J. Chem.* **1982**, *60*, 801. (b) Furukawa, J.; Kobayashi, E.; Nagata, S.; Moritani, T. *J. Polym. Sci., Poly. Chem. Ed.* **1974**, *12*, 1799. (c) Kuran, W.; Pasynkiewicz, S.; Florjanczyk, Z.; Lusztyk, E. *Makromol. Chem.* **1976**, *177*, 2627.

(29) Bonnesen, P. V.; Puckett, C. L.; Honeychuck, R. V.; Hersh, W. H. *J. Am. Chem. Soc.* **1989**, *111*, 6070.

(30) (a) Satchell, N. P. D.; Satchell, R. S. *Chem. Rev.* **1969**, *69*, 251. (b) Satchell, N. P. D.; Satchell, R. S. *Q. Rev., Chem. Soc.* **1971**, *25*, 171.

Table III. Comparison of Lewis Acid Strengths[a]

Lewis acid	$\Delta\delta$ (ppm)	ref
BBr_3	1.49	28a
$AlCl_3$	1.23	28a
$[HC(py)_3W(NO)_2](SbF_6)_2$	1.19	
BF_3	1.17	28a
$[HC(py)_3Mo(NO)_2](SbF_6)_2$	1.05	
$TiCl_4$	1.03	28a
$[Me_3P(CO)_3(NO)W]^+$	0.93	29
$SnCl_4$	0.87	28a
$CpMo(CO)_3^+$	0.70	29
Et_3Al	0.63	28a
$CpFe(CO)_2^+$	0.54	29

[a] Based upon the relative downfield shift of H_3 upon coordination of crotonaldehyde.

dienophile such as methyl acrylate is used, considerable polymerization of butadiene takes place, forming a viscous oil, which is insoluble in nitromethane-d_3. The scope of the catalytic properties of these Lewis acids and the mechanistic implications will be the subject of further investigation.

η^1 versus η^2 Binding. The $[HC(py)_3M(NO)_2]^{2+}$ Lewis acids have been shown to be strong and relatively hard acids. No η^2 binding was directly observed with aldehydes, ketones, or esters. In the case of aldehydes, separate signals for free and bound aldehyde were observed and the NMR chemical shifts were the primary evidence for η^1 binding. Since no separate resonance for an η^2-bound aldehyde was observed, it is possible that such a species was present in low concentration and exchanging rapidly with either the free or η^1-bound aldehyde. Although at lower temperatures a separate resonance for an η^2-bound species was never observed, in some instances (low free aldehyde concentration) broadening of the "free" aldehyde resonance was observed, even at room temperature. When the temperature was from −40 °C to +40 °C for benzaldehyde with $[HC(py)_3W(NO)_2]^{2+}$, the "free" resonance progressed from a fairly narrow line to a broad resonance (7 Hz) at 10 °C and back to a narrower line, yet it did not show an appreciable shift (~0.02 ppm).[31] This result is consistent with exchange between a very low concentration species and free aldehyde. We attribute this behavior to relatively facile exchange between free aldehyde and a weakly bound η^2-aldehyde species in very low concentration (<1%). Since no broadening was observed in the η^1-aldehyde resonance, the η^1-aldehyde cannot be interconverting with the η^2 complex rapidly. Therefore, we conclude that the rapid rearrangements between syn and anti isomers in an η^1 complex cannot involve an η^2 intermediate in these complexes. In this context, we favor a transition state in which the metal remains in the CHO plane during the "migration from one oxygen lone pair to the other". By analogy to theoretical analyses for main-group Lewis acid migrations,[32] this path appears more favorable than one involving out-of-plane structures. The relatively low barrier to this migration suggests that one consider a process involving continual rehybridization of the lone-pair orbital throughout this motion to maintain a strong σ bond to the metal. Hence, the transition state would involve an sp donor orbital with the lone pair in a p orbital, rather than both pairs utilizing the sp^2 hybrids of the ground states.

Similar evidence for a small fraction of η^2-ester exchanging with free ester, but not with η^1-ester, can be observed in the spectra of the methyl acetate adduct (Figure 5).[33] This suggests that the path for syn–anti migration of the metal in ester complexes is similar to that described for the aldehyde adducts.

Acknowledgment is made to the donors of the Petroleum Research Fund, administered by the American Chemical Society, for support of this research. We also thank Drs. D. L. White, C. Blankenship, L. Maheu, and B. Whitmore for their contributions to the development of better procedures for the preparation of $HC(py)_3$.

(31) The amount of the shift varied with the relative concentration of free aldehyde. The broadening was usually clearly observable at high fields. At lower fields (<250 MHz) and higher relative concentrations ([aldehyde]:[complex] >2), sharp resonances were observed for the "free" aldehyde.
(32) LePage, T. J.; Wiberg, K. B. *J. Am. Chem. Soc.* **1988**, *110*, 6642.
(33) Ma, Y. Ph.D. Dissertation, Yale University, New Haven, CT, May 1989.

Reversible Two-Electron–One-Proton Systems in the Ring-Centered Oxidation of Metalloporphyrins Bearing Secondary Amide-Linked Superstructures

Asma El-Kasmi,[1a] Doris Lexa,[1a] Philippe Maillard,[1b] Michel Momenteau,[1b] and Jean-Michel Savéant*,[1a]

Contribution from the Laboratoire d'Electrochimie Moléculaire de l'Université de Paris 7, Unité Associée au CNRS 438, 2 Place Jussieu, 75251 Paris Cedex 05, France, and the Institut Curie, Section de Biologie Unité Inserm 219, 91405 Orsay, France. *Received August 6, 1990*

Abstract: Complexes of porphyrins derived from tetraphenylporphyrin by substitution of the ortho position of the phenyl rings by secondary amide groups in a basket-handle or picket configuration undergo a reversible two-electron oxidation whatever the nature of the central metallic ion, Cu^{2+}, Zn^{2+}, Ni^{2+}, Fe^{3+}, Co^{3+}, in solvents such as 1,2-dichloroethane, methylene chloride, and benzonitrile. The reaction mechanism is investigated by cyclic voltammetry (as a function of the scan rate and the addition of a base or an acid) and UV–vis–near-IR and Fourier transform IR thin-layer spectroelectrochemistry. The reaction product is an endogeneous isoporphyrin resulting from the formation of an oxazine ring formed upon condensation of a meso carbon of the porphyrin dication with the oxygen of the amide group. The same reaction occurs with tertiary amide substituents, but in the case of secondary amide the concomitant loss of the amide proton facilitates the formation of the isoporphyrin. It thus drives the uphill disproportionation of two cation radicals to the right-hand side to such an extent that the uptake of the two electrons takes place at nearly the same potential. The reduction of the internal isoporphyrin is also a two-electron reaction at low scan rates with both the secondary and tertiary amide substituted compounds. The two-electron character of the isoporphyrin reduction is the result of an autocatalytic process in which the porphyrin cation radical serves as redox catalyst.

Metalloporphyrins bearing superstructures attached to the porphyrin ligand by means of secondary amido groups have been extensively employed to mimic the role of the proteinic environment of the prosthetic group of hemoglobin and myoglobin in

0002-7863/91/1513-1586$02.50/0